ELSEVIER

Thermochimica Acta 246 (1994) 153–165

thermochimica acta

Polymer melting: simulation and experimental results from a single melting peak model system

Ge Wang, Ian R. Harrison*

Polymer Science Program, Department of Materials Science and Engineering, The Pennsylvania State University, 325 Steidle Building, University Park, PA 16802, USA

Received 3 November 1993; accepted 27 February 1994

Abstract

Experimental polymer melting as observed in differential scanning calorimetry (DSC) is generally complicated by the influence of lamellar thickness distributions and/or reorganizational effects. Idealized polymer melting in the absence of such effects is critical both for a basic understanding of the DSC results and for decoupling instrumental from sample size broadening effects. A model system which does not have the mentioned complicating effects was developed, consisting of a polyethylene–indium powder mixture. The melting behavior of this model system was experimentally investigated and simulated by a "shell model" that treats melting in a DSC sample as the melting of a series of shells. All of the parameters in the model are obtained experimentally; none is adjustable. The simulation was generally quite satisfying, although a somewhat greater deviation was observed for extreme heating rates (1°C min^{-1} and 40°C min^{-1}). In addition to the "shell model" simulation, a single Gray type melting peak was also found useful in approximating the experimental curve.

Keywords: DSC; Melting; Model; Polymer

1. Introduction

One approach to differential scanning calorimetry (DSC) is to measure the rate of heat flow into a sample and a reference while attempting to maintain identical temperatures as the sample and reference are heated or cooled. The difference in

* Corresponding author.

SSDI 0040-6031(94)01782-C

rate of heat flow for the sample compared with the reference is plotted against programmed temperature or time. Changes in heat capacity, chemical reactions and physical transitions can be detected, as these events affect the rate of heat flow. DSC is widely used in the thermal analysis of organic and polymeric materials, as many important parameters such as glass and melting temperatures, heats of fusion and heats of crystallization can be conveniently obtained from DSC curves.

Despite the broad appeal of DSC, the development of further applications that demand more accurate information is often hampered by thermal lag problems associated with instrumental and sample size effects. One example of a general application involves calculation of partial peak area to determine kinetic parameters, purity or lamellar thickness distributions. A prerequisite for obtaining reliable results from these calculations is to acquire accurate partial peak areas corresponding to specific temperatures or times. It is difficult to obtain this information because melting peaks are broadened owing to "thermal lag". Attempts have been made to correct for thermal lag using the leading edge of a reference material's melting peak as a guide [1]. This method has severe practical limitations, as it requires the thermal conductivity for reference and sample to be matched. More importantly, the method is inherently flawed because it assumes a constant thermal resistance throughout the sample. In fact, we have previously shown that within normal sized polymer DSC samples (10–20 mg) thermal resistance between sample center and sample surface may differ by a factor of 4 [2], and other authors have reported somewhat larger differences [3]. Currently there are no satisfactory methods that can be used to remove thermal lag, or to separate true peak shape from sample and instrumental effects; this paper is directed towards achieving that goal.

It is clear that sample size effects must be considered if one wants to eliminate thermal lag. Size effects result from the low thermal conductivity of polymers, which causes temperature gradients within DSC samples. As the programmed temperature is increased, only material that is in contact with the sample pan can change temperature responsively [2]. Material away from the pan surface, in the interior of the sample, will not be able to respond at the same rate; this behavior results in a complicated overall thermal response. Even for pure materials of low molecular weight, the melting peak is not a "spike", but rather a peak with finite width and a particular shape. In other words, all DSC melting peaks are broadened and points on the melting curve are not interpretable as true melting temperatures. These deviations become more severe as sample size increases.

In addition, the melting behavior of polymers is far more complicated than that of low molecular weight materials. Within a polymer there may exist a distribution of lamella thicknesses leading to a distribution of melting temperatures. Annealing and/or recrystallization may also occur while a polymer is being heated towards and through the melting temperature range; this "reorganization" can lead to broadened or multiple peaks. To extract the "true" melting curve from experimental data we need to first understand how a sample having a single lamella thickness would behave in a DSC pan in the absence of the reorganizational complications mentioned above. In this work, we have experimentally studied and simulated the DSC melting curves of a model polymer sample composed of polyethylene (PE)

and indium powder. Indium powder was uniformly mixed with polyethylene; the indium simulates polymer crystals having a single thickness lamella and therefore a single melting temperature and, furthermore, no annealing or remelting of indium occurs on heating. In all cases we are recording the melting of indium in an amorphous PE matrix; PE melts at a lower temperature than indium.

In this paper, we first review Gray's theoretical model [4] concerning the melting peak shape for a very small sample. This model is then adapted to describe the melting curves of normal sized polymer samples. A computer program based on an adaptation of Gray's theory was developed to simulate experimental DSC melting peaks. Both computer simulated and experimentally obtained DSC melting curves for different heating rates are presented and discussed.

2. Experimental

2.1. Polyethylene–indium powder samples

Indium powder (size 150 mesh, purity 99.99%) was used to prepare a polymer–indium mixture with high density polyethylene (HDPE). To mix indium powder and HDPE, the powder was evenly spread on HDPE blown film and then covered by another HDPE film. This sandwich was placed between Teflon-coated aluminum sheets and pressed at 150°C. After pressing, the newly formed PE–indium powder film was folded once in half and re-pressed. This latter process was repeated ≈ 25 times. The final film was inspected using an optical microscope to ensure uniform distribution of indium within the PE matrix. In this way approximately 5% by weight of indium was incorporated into HDPE film. To make sure that the sample made good contact with the sample pan, a paper hole punch was used to cut the PE–indium film into circular pieces which exactly fitted aluminum DSC pans. The sample pan bottom was flattened after sealing.

2.2. Polyethylene–indium foil samples

High density PE blown film with a thickness of ≈ 0.08 mm was punched into circular pieces using a paper hole punch. The circular film had a diameter corresponding to the inner diameter of our DSC aluminum pans. The average weight of one circular layer of PE film was ≈ 2 mg. Thin indium foil (thickness 0.02–0.03 mm, purity 99.999%) was prepared by pressing 0.1 mm indium foil between clean glass slides separated by a razor blade edge. The indium foil samples had a circular shape of area ≈ 3 mm^2. Samples with various sandwich structures were made by carefully stacking indium foil and PE films into DSC aluminum pans in different sequences. Three sample configurations represented by "In/k PE/In/k PE", "k PE/In/k PE" and "In/k PE" are shown in Fig. 1; k is the number of PE films used and stacking sequence is read from left to right.

All DSC tests were performed on a Perkin Elmer DSC 7 instrument, which was calibrated at 10°C min^{-1} against a normal indium sample (≈ 5 mg). Argon was

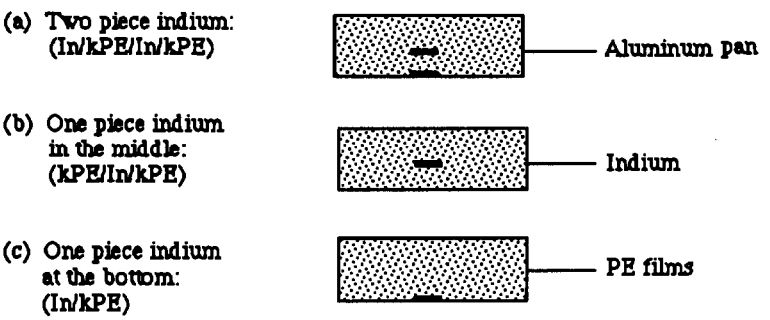

Fig. 1. Sample configurations.

used as the purge gas. Experimental data were transferred from the Perkin Elmer computer into PC readable ASCII format data. A computer program was written in C language to analyze experimental DSC data and also to create computer simulated DSC curves.

3. Theoretical DSC peak analysis

The theoretical development of peak shape has been presented in an earlier paper [5], but is included here for completeness. For very small samples, a model for melting peak shape has been developed by Gray based on energy conservation and Newton's law. The melting peak shape for such a small sample has been shown to consist of two half-peaks; the first half-peak has a straight line slope and the second half-peak shows an exponentially decaying curve (Fig. 2). The following equations describe the two half-peaks.

For the first half-peak:

$$\frac{dq}{dt} = \frac{1}{R}\frac{dT_p}{dt}t \tag{1}$$

For the second half-peak:

$$\frac{dq}{dt} = \left(\frac{dq}{dt}\right)_{max} \exp\left(\frac{-t}{RC_s}\right) \tag{2}$$

where dq/dt is the heat flow rate, R is the thermal resistance, C_s is the total sample heat capacity, dT_p/dt is the heating rate, and t is time.

It should be noted that sample melting is complete at the peak maximum and not at the end of the peak [5]. With reference to Fig. 2, the above statement means that melting starts at point a and ends at point b. The whole melting enthalpy is thus represented by the summation of areas A and C. Since it is experimentally difficult to determine area C, the normal procedure in obtaining melting enthalpy is to measure the total peak area (A + B). The justification for so doing comes from the fact that area C equals area B; both B and C are equal to $(dq/dt)_{max}RC_s$.

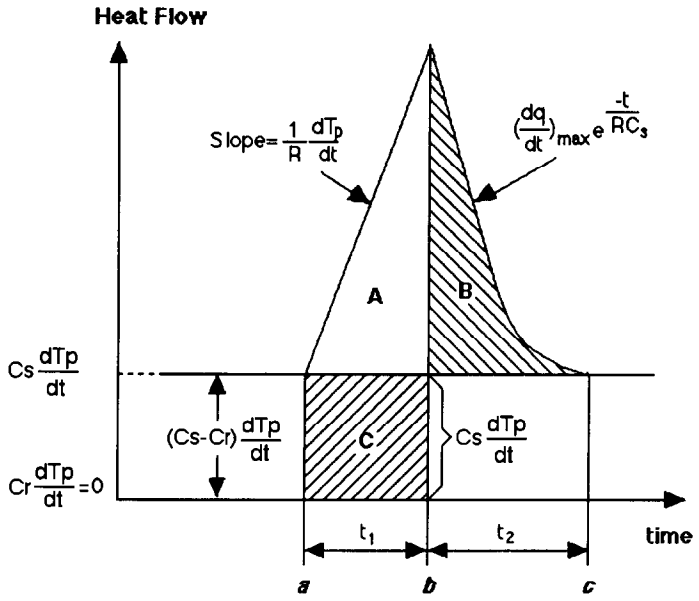

Fig. 2. Schematic representation of a sharp transition DSC peak.

From Eqs. (1) and (2), we see that heating rate affects the slope of the first half-peak. As the heating rate increases, the slope becomes steeper and the whole melting peak becomes narrower. In order to define and describe the effects of heating rate on overall melting peak shape, we need to determine parameters such as peak height $(dq/dt)_{max}$, the time needed for the crystalline material in the sample to melt (t_1) and the time needed for the sample temperature to catch up with the programmed temperature (t_2). Theoretically, t_2 will be infinitely long; however, for practical purposes, t_2 can be defined as the time for dq/dt to fall below 1% of its maximum value. Regardless of how peak shape changes, the total energy required to melt the same amount of material remains constant, i.e. peak area is a constant. With this in mind, we can determine how heating rate affects t_1 and t_2.

The total energy to melt the material (ΔH) can be obtained by integration from the onset to the end of the melting, i.e. from $t = 0$ to $t = t_1$

$$\Delta H = \int \frac{dq}{dt}\, dt = \frac{dT_p}{dt}\frac{t_1^2}{2R} + C_s \frac{dT_p}{dt} t_1 \tag{3}$$

Solving this equation, we find

$$t_1 = RC_s\left[\sqrt{1 + \frac{2\Delta H}{RC_s^2 \dfrac{dT_p}{dt}}} - 1\right] \tag{4}$$

Rearranging Eq. (2) gives

$$t_2 = RC_s \ln\left[\frac{(dq/dt)_{max}}{\Delta}\right] = RC_s \ln(100) \tag{5}$$

where Δ represents the value dq/dt where the peak tail can be considered essentially returned to baseline; in this case Δ is set at 1% of the difference between $(dq/dt)_{max}$ and the baseline value.

Peak height from baseline can be calculated by replacing t in Eq. (1) with t_1 from Eq. (4), then

$$\left(\frac{dq}{dt}\right)_{max} = \frac{dT_p}{dt} C_s \left[\sqrt{1 + \frac{2\Delta H}{RC_s^2 \frac{dT_p}{dt}}} - 1\right] \tag{6}$$

4. Computer simulation

DSC melting curves change appreciably with increases in sample size, and an understanding of these changes is crucial in simulating real melting behavior. For normal sized samples, previous experiments have clearly shown that there are considerable variations in thermal resistance within the sample [2]. In contrast, the theoretical analysis presented above is based on the assumption that sample size is so small that thermal resistance is constant throughout.

Because of the high thermal conductivity of aluminum pans and the relatively low thermal conductivity of polymers, it is reasonable to assume that heat flows into the sample from all directions. Further, in order to model the melting transition of a normal sized polymer sample, we envision that such a sample consists of many thin shells (see Fig. 3), each of which is small enough to be treated as an independent small sample with a Gray type peak shape. Summation of all the small melting peaks makes up the overall observed DSC melting peak for the sample.

To generate the melting peak for each thin shell, we need to know four parameters: dT_p/dt, ΔH, R and C_s. The heating rate (dT_p/dt) is known and the heat of fusion of each shell (ΔH_n, mJ) is the product of the shell volume (ΔV_n, mm^3) and the experimentally determined heat of fusion (ΔH, mJ mm^{-3}) for the whole sample. Assuming a perfectly circular disk geometry for the DSC sample, ΔV_n and ΔH_n can be calculated based on sample thickness and the total number of shells (N).

As an approximation, we assume that both thermal resistance R and heat capacity C_s vary linearly with the distance from the sample surface to the middle of the sample. The values of R and C_s at the bottom surface (R_b and C_b) and at the middle of the sample (R_m and C_m) can be obtained from tests on PE–indium foil sandwich samples [2]. So we may write

$$R_n = R_b + \frac{R_m - R_b}{N}(n + 1) \tag{7}$$

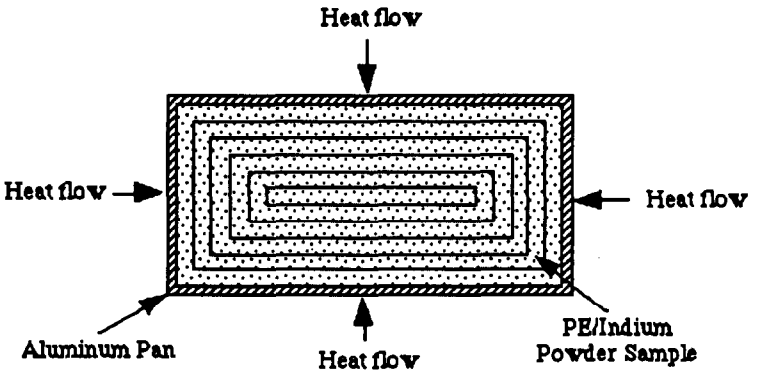

Fig. 3. Schematic representation of a cross-section of the sample divided into many small shells.

$$C_n = C_b + \frac{C_m - C_b}{N}(n+1) \tag{8}$$

where R_n and C_n are the resistance and the heat capacity respectively of the nth shell and n varies from 0 to $N-1$.

After generating all the thin shell melting peaks using Gray's model, we need to add them to form the overall DSC melting peak of the whole sample. To do this, we need to know how to place the melting peaks on the time axis. Since melting of each thin shell ends at the end of the first half-peak [4], it is tempting to position those peaks such that the onset of melting of a shell starts at the point where melting of the previous outer shell ends. This is illustrated in Fig. 4, where the first melting peak ends at t_1, which is also the start of the second melting peak, which then ends at t_2.

In an earlier study on PE–indium foil sandwich structures, we had noticed that this sort of placement for co-addition gives general agreement with regard to overall shape [2]. However, even better fit is obtained when the contributing peaks are moved closer together (see Fig. 5). This is equivalent to saying that melting from an inside shell starts before the outside shell has completely finished melting. This idea is shown schematically in Fig. 6 on a plot of temperature versus time. Reference temperature (T_r) increases linearly with time; the outer shell temperature (T_1) is offset from T_r for clarity and the temperature of the inner shell (T_2) or foil lags behind T_1. At time A the outer shell starts to melt, and its temperature stays constant until melting is complete at point C. While the outer shell is melting, the inner shell "sees" a constant temperature source, as opposed to a gradually increasing temperature which it experienced previously. The question then remains, at what point does T_2 catch up with T_1? It seems reasonable that T_2 will not catch up with T_1 at time B, since we do not expect the inner shell to continue to heat up at the same rate that it experienced before the outer shell melted. The placement shown in Fig. 4 is correct only if T_2 catches up with T_1 at point C. Earlier experiments [2] suggest that T_2 reaches the melting point before point C, say at point D.

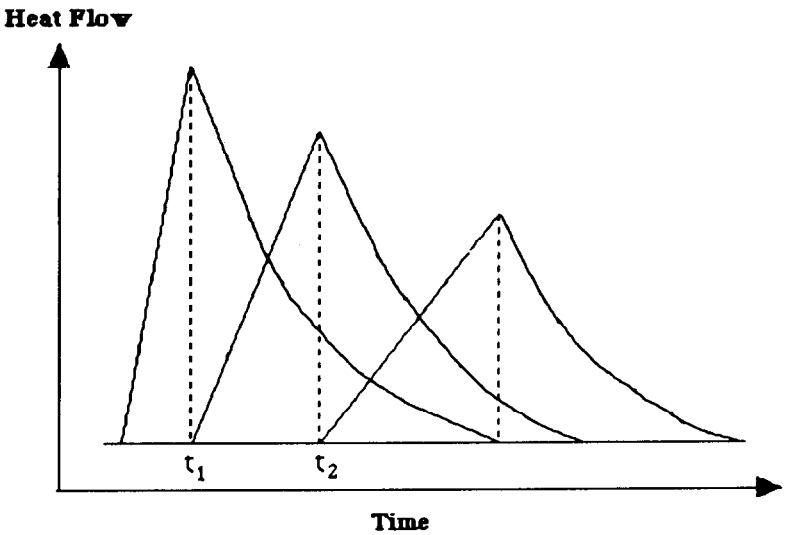

Fig. 4. Schematic illustration of one way to add small Gray type melting peaks of thin shells.

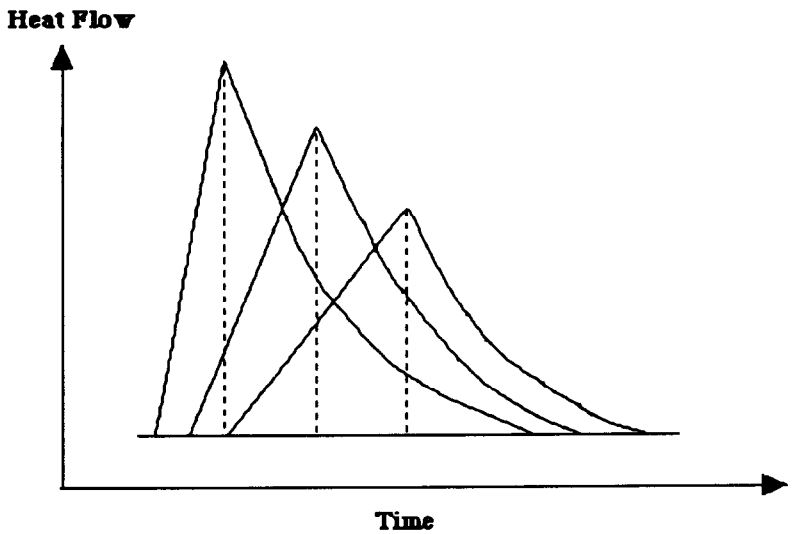

Fig. 5. Schematic representation of a more realistic method for adding small melting peaks of thin shells.

5. Results and discussion

Before comparing simulated DSC curves with experimental ones run at different heating rates, it is worth noting an unusual melting behavior for the thin shells. Fig. 7 displays a typical simulated melting peak resulting from summation of all the thin

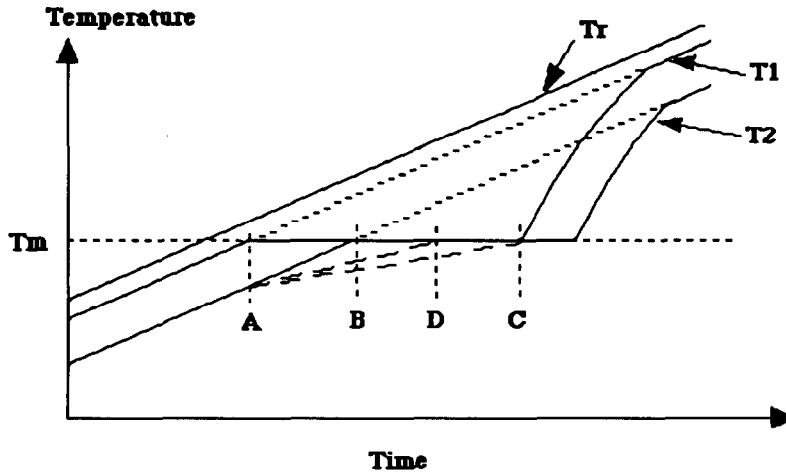

Fig. 6. Schematic representation of the temperature profile between two adjacent shells. T_r is the temperature of the reference cell. T_1 and T_2 are the temperatures of the outer and the inner shell respectively.

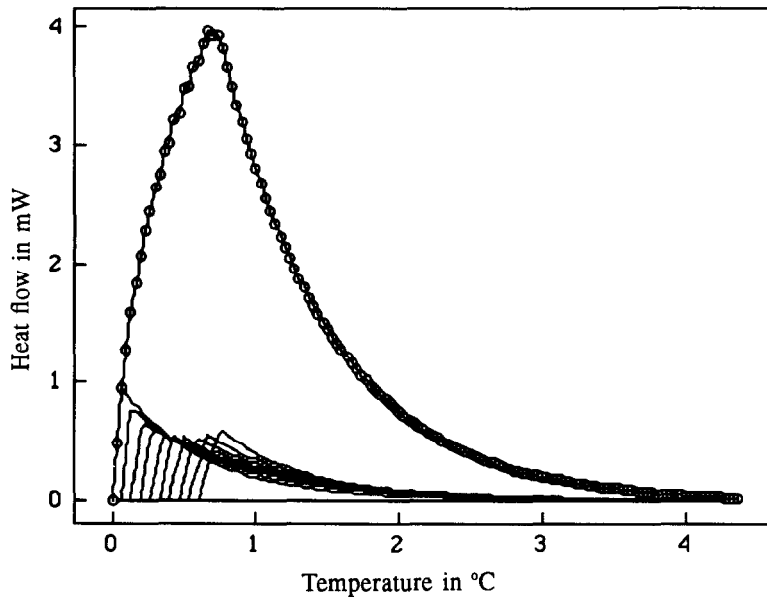

Fig. 7. A typical computer simulated overall melting peak and its 10 shell melting peaks.

shell melting peaks. Note that shell melting peak height is not monotonically reduced with decreasing shell volume. This unanticipated behavior can be explained by examining Eq. (6). It is clear from Eq. (6) that a combination of three parameters ($\Delta H/RC_s^2$) plays the determining role in establishing peak height. Although heating

rate also affects peak height it is a constant in this case. Peak height decreases as shell volume and therefore ΔH decreases and thermal resistance R increases. This effect is demonstrated by decreased melting peak heights for the first seven shells. However, as shell volume decreases the total effective heat capacity (C_s) also decreases, and therefore peak height increases. Alternative explanations have been proposed for apparent heat capacity changes [3,6]. For interior shells with decreasing size and heat capacity, the squared C_s term starts to influence peak height more effectively than changes in ΔH and R.

Melting peak simulation for a real polymer system requires knowledge of the four parameters discussed previously and the time offset for each shell (Fig. 6). As discussed earlier, the four heat capacity and thermal resistance parameters C_b, C_m, R_b and R_m can be experimentally determined from sandwiched PE–indium foil samples having the same sample heights as the PE–indium powder samples and run under the same conditions. Although the time offset for each shell cannot be measured directly from experiment, it can be approximated in the following way. The time interval between melting of the middle and the bottom of a sample can be directly measured from PE–indium foil samples, and it should be equal to the summation of all time intervals between thin shells. Assuming equal time intervals between each of N shells, we can reasonably estimate individual shell offset time. Without a reasonably accurate estimation of this parameter simulation would not be possible, as different time offsets result in different shaped melting peaks. Fig. 8 shows the effect of time offset on the overall DSC melting peak. As time offset increases, peak height decreases and peak width increases.

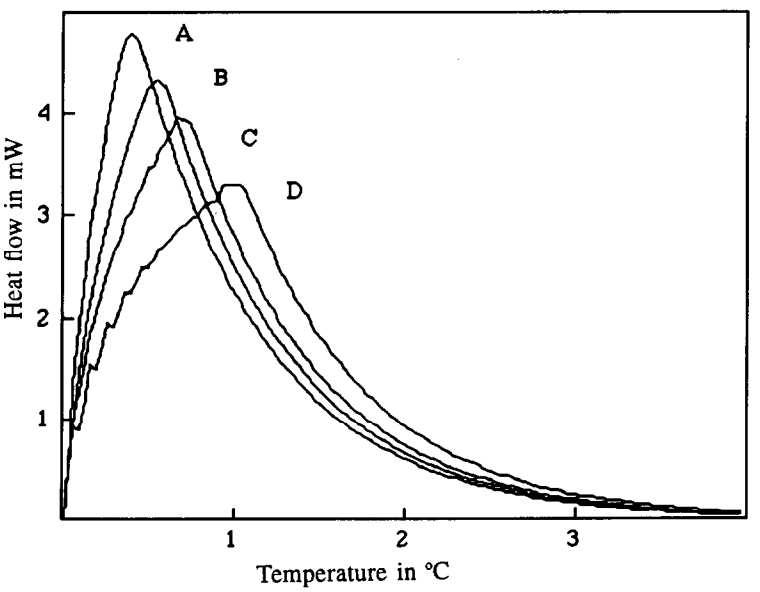

Fig. 8. Simulated curves for a 10 shell model obtained from different time offsets between the bottom and the center of the sample. A, 1.8 s; B, 2.7 s (determined from experimental data); C, 3.6 s; D, 5.4 s. The heating rate used in the above simulations was 10°C min^{-1}.

Table 1
Parameters derived from PE–indium foil samples

Heating rate	R_b/(°C mW^{-1})	R_m/(°C mW^{-1})	C_b/(mJ K^{-1})	C_m/(mJ K^{-1})	Total Δt/(s)
1°C min^{-1}	0.058	0.225	68.0	20.0	8.76
5°C min^{-1}	0.062	0.238	60.5	15.5	3.85
10°C min^{-1}	0.071	0.258	51.0	14.0	2.64
20°C min^{-1}	0.095	0.319	37.5	11.5	2.55
40°C min^{-1}	0.162	0.399	21.0	8.0	1.98

In the following simulations for real DSC melting curves, the time offset between each shell was determined experimentally from PE–indium foil samples and was not adjusted to fit the data from PE–indium powder samples. Estimated and experimentally measured parameters used for a variety of simulations are listed in Table 1. Experimental DSC curves for PE–indium powder samples and simulated curves are shown in Fig. 9. In general, the simulations are quite satisfying, especially for those curves with heating rates of 5, 10 and 20°C min^{-1}. Greater deviation is seen between simulated and experimental curves for heating rates of 40°C min^{-1} and 1°C min^{-1} (on an appropriate scale).

One important difference between simulated and experimental DSC curves is that, in all cases, simulated melting peaks rise abruptly, whereas experimental DSC curves rise in a more gradual fashion. This observation suggests that the first shell for PE–indium powder samples might possess significantly higher thermal resistance than the R_b derived from PE–foil experiments, which is close to the minimum thermal resistance value R_0.

Experimental curves shown in Fig. 9 can also be fitted approximately with just a single Gray type curve. An example is shown in Fig. 10 for a sample heated at 10°C min^{-1}. In this latter case the fitted R and C are the average of experimental bottom and middle values of R and C respectively for a comparably sized PE–indium foil sample. Such an observation suggests that it is reasonable to model the melting peak of a normal sized semicrystalline polymer by using R and C averages from a single polymer–indium foil experiment. Although no meaningful theoretical explanation is currently available for this kind of averaging operation, this approach does provide a quick way to obtain the shape of the melting peak free from lamella thickness distribution effects. In essence, such a melting curve represents "instrumental broadening" for this size of sample. Considering that the ultimate simulation for a real polymer melting peak will be based on the summation of many such single lamellar melting peaks, the time saved and greater ease of calculation would be significant.

6. Summary and conclusions

A model system made from a mixture of PE–indium powder was used to simulate the melting process for a simplified case where a polymer contains only

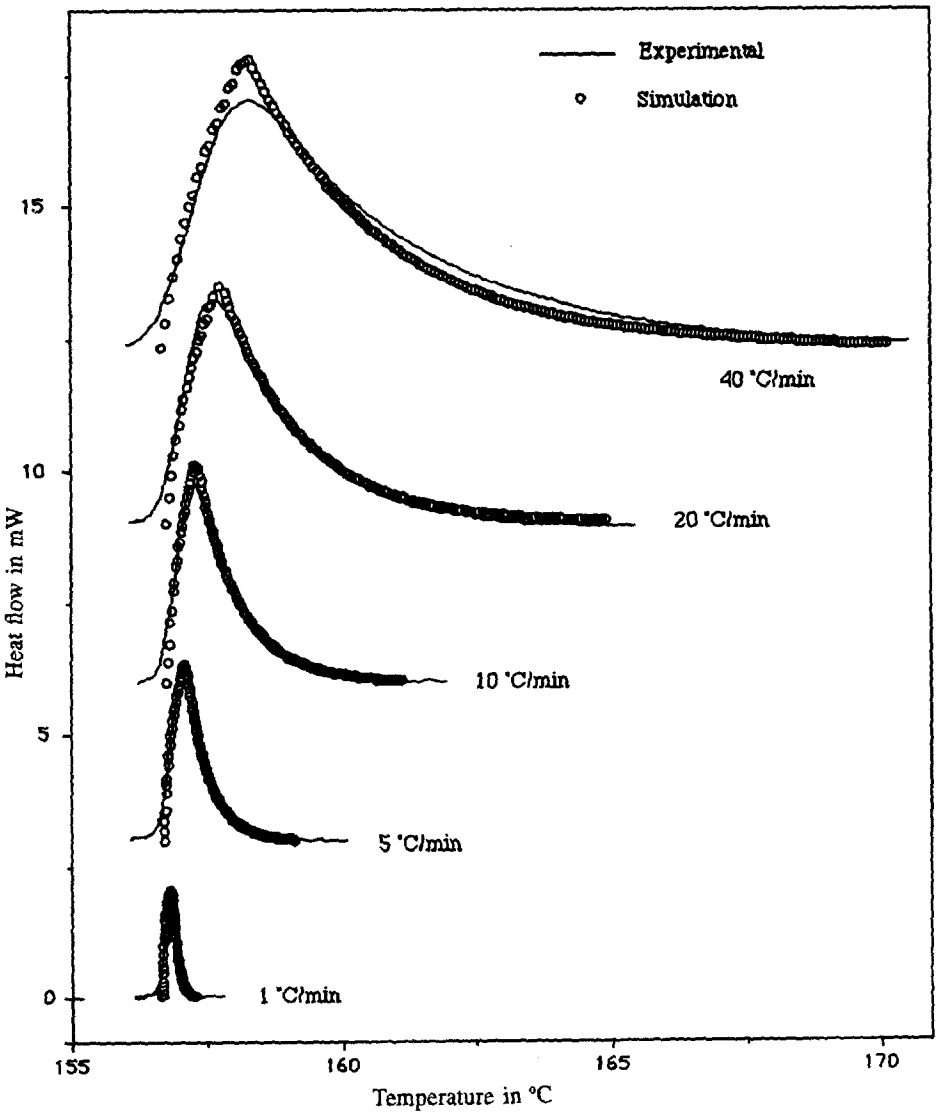

Fig. 9. Comparison between experimental and simulated DSC curves for different heating rates.

one crystalline component. This simplified system is necessary to remove the influence of other effects such as lamellar thickness distribution and reorganization.

Simulation of melting peaks for normal sized DSC samples was based on a "shell model" that treats the melting process in a DSC sample as a series of melting shells. The whole sample is melted, shell by shell, from the surface shell to the center of the sample, and each shell is so small that its melting peak can be described by Gray's equations. As shells are not physically separated in the sample, one shell starts to

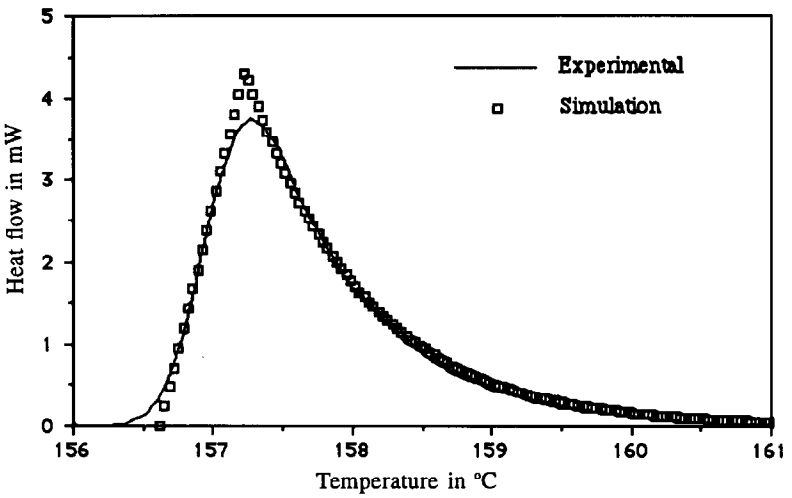

Fig. 10. Comparison between experimental DSC and a simulated single Gray type curve for a PE–indium powder sample tested at a heating rate of 10°C min^{-1}. Other parameters used: R = 0.14°C mW^{-1}, C = 36 mJ^{-1}.

melt before the neighboring outer shell has completed its melting. This problem was dealt with by using an averaged time offset estimated from PE–indium foil experiments. All other parameters used in the simulation were obtained from similar experimental data. In general, the simulation was quite satisfying, although a somewhat greater deviation was observed for extreme heating rates (1 and 40°C min^{-1}).

In addition to the "shell model" simulation, which is basically a summation of all shell melting peaks, we also found that a single Gray type melting peak can be used to approximate the experimental curve. In this case R and C_s for the Gray model are averages of thermal resistance and heat capacity values found from PE–indium foil experiments. The physical meaning of this latter approach is unclear; however, it does provide a fast way to peak simulation. Such an easy simulation will be highly desirable in defining real polymer melting processes which include lamella thickness distributions and reorganization.

References

[1] Thermal Analysis Newsletter, No. 5, Perkin-Elmer Corp., Norwalk, CT.
[2] G. Wang and I.R. Harrison, Thermochim. Acta, in press.
[3] J.H. Flynn, in R.S. Porter and J.F. Johnson (Eds.), Analytical Calorimetry, Vol. 3, Plenum Press, New York, 1974, p. 39.
[4] A.P. Gray, in R.S. Porter and J.F. Johnson (Eds.), Analytical Calorimetry, Vol. 1, Plenum Press, New York, 1968, p. 209.
[5] G. Wang and I.R. Harrison, Thermochim. Acta, in press.
[6] J.H. Flynn and D.M. Levin, Thermochim. Acta, 126 (1988) 93.